Food and Chemical Toxicology 181 (2023) 114107

Contents lists available at ScienceDirect

Food and Chemical Toxicology

journal homepage: www.elsevier.com/locate/foodchemtox

Low concentrations of antimony impair adipogenesis and endoplasmic reticulum homeostasis during 3T3-L1 cells differentiation

Maria Sofia Molonia [a,b], Claudia Muscarà [a], Antonio Speciale [a,*], Federica Lina Salamone [a], Gregorio Costa [c], Grazia Vento [d], Antonella Saija [a,1], Francesco Cimino [a,1]

[a] Department of Chemical, Biological, Pharmaceutical and Environmental Sciences, University of Messina, Viale F. Stagno D'Alcontres 31, 98166, Messina, Italy
[b] "Prof. Antonio Imbesi" Foundation, University of Messina, 98100, Messina, Italy
[c] Department of Human Pathology in Adult and Developmental Age, University of Messina, 98125, Messina, Italy
[d] Department of Experimental Medicine (DIMES), University of Genova, 16132, Genoa, Italy

ARTICLE INFO

Handling Editor: Dr. Bryan Delaney

Keywords:
Antimony
Metalloestrogens
Endocrine-disrupting chemicals
Adipocytes
Lipid accumulation
Endoplasmic reticulum stress

ABSTRACT

Antimony (Sb) is a metalloid widely present in plastics used for food contact packaging, toys and other household items. Since Sb can be released by these plastics and come into contact with humans, health concerns have been highlighted. The effect of Sb on human tissues is yet controversial, and biochemical mechanisms of toxicity are lacking. In the present study, the effect of very low nanomolar concentrations of Sb(III), able to mimicking chronic human exposure, was evaluated in 3T3-L1 murine cells during the differentiation process. Low nanomolar Sb exposure (from 0.05 to 5 nM) induced lipid accumulation and a marked increase in C/EBP-β and PPAR-γ levels, the master regulators of adipogenesis. The Sb-induced PPAR-γ was reverted by the estrogen receptor antagonist ICI 182,780. Additionally, Sb stimulated preadipocytes proliferation inducing G2/M phase of cell cycle and this effect was associated to reduced cell-cycle inhibitor p21 levels. In addition to these metabolic dysfunctions, Sb activated the proinflammatory NF-κB pathway and altered endoplasmic reticulum (ER) homeostasis inducing ROS increase, ER stress markers XBP-1s and pEIF2a and downstream genes, such as Grp78 and CHOP. This study, for the first time, supports obesogenic effects of low concentrations exposure of Sb during preadipocytes differentiation.

1. Introduction

Antimony (Sb) is a metalloid existing in a variety of oxidation states (-3, 0, +3 and + 5); its toxicity highly depends upon chemical form and oxidation state with +III compounds exerting greater toxicity than + V compounds (Lai et al., 2022; Li et al., 2018).

Sb is used as a synergist together with flame retardants for use in plastics, rubber, paints, paper, textiles, and electronics, and as a catalyst in the manufacturing of plastics (Snedeker, 2014). A key consideration is that plastic additives, like also Sb, are not chemically bound to the polymer so that when plastic articles are subjected to stressful or different conditions from their use, these additives can be removed or released from the plastic. Potential Sb exposure routes include ingestion [e.g., drinks in polyethylene terephthalate (PET) or polyvinyl chloride (PVC) containers or from children's toys], and dermal contact or inhalation (primarily release from flame retardants used in upholstered furniture) (Brandsma et al., 2022; Filella, 2020; Li et al., 2018). Therefore, the interest in the presence of Sb in consumer products, which are mostly plastics, is increasing.

Health concerns for Sb exposure arise in particular for the potential mutagenic and carcinogenic risks, especially at the pulmonary level following occupational exposure, although antimony carcinogenic properties remain under debate and the mechanisms potentially involved need to be explored (Boreiko and Rossman, 2020; Lou et al., 2021; Saerens et al., 2019). Sb has been reported to cross the cell membrane via aquaglyceroporins and metalloid transporters, and to interact with biomolecules, in particular affecting the expression and synthesis of functional proteins (Lai et al., 2022). However, the effect of antimony on human organs and tissues is yet controversial, especially since deep information about specific biochemical mechanisms of

* Corresponding author.
E-mail addresses: mmolonia@unime.it (M.S. Molonia), cmuscara@unime.it (C. Muscarà), specialea@unime.it (A. Speciale), federica.salamone@studenti.unime.it (F.L. Salamone), gregorio.costa@unime.it (G. Costa), grazia.vento@edu.unige.it (G. Vento), asaija@unime.it (A. Saija), fcimino@unime.it (F. Cimino).
[1] These authors share the senior authorship.

https://doi.org/10.1016/j.fct.2023.114107
Received 2 May 2023; Received in revised form 21 September 2023; Accepted 16 October 2023
Available online 18 October 2023

toxicity is lacking. Additionally, Sb concentrations in human blood usually are very close to the detection limit of the analytical techniques used leading to an overestimation in the concentrations reported (Filella et al., 2013).

Recently metal ions have been investigated as capable of interfering with estrogen action, representing a new class of inorganic xenobiotics (both cations and anions) named metalloestrogens (Darbre, 2006). Sb has been reported to show high estrogenicity in *in vitro* assays (Choe et al., 2003); furthermore, Zhang and coworkers (Zhang et al., 2018) have hypothesized that antimony could promote prostate cancer progression through mimicking androgen activity. These observations support the role of this metal as an environmental endocrine disruptor.

Endocrine-disrupting chemicals (EDCs) are exogenous compounds that interfere with the normal function of endocrine system and thus increase the risk of adverse health outcomes, including cancer, reproductive impairment, cognitive deficits, and metabolic dysfunction such as obesity (La Merrill et al., 2020). The role of EDCs in metabolic syndrome and obesity is centered on a group of EDCs known as obesogens, able to promote adipogenesis and cause weight gain. In particular, *in vivo* studies reported that bisphenol-A (BPA), phthalates and tributyltin, found in many consumer plastic products, affect adipose tissue by altering programming of fat cell development, increasing energy storage in adipocytes, and interfering with neuroendocrine control of appetite and satiety (Darbre, 2017). At a molecular level, obesogens can interfere with transcriptional factors that modulate lipid flux and/or adipocyte differentiation, such as the peroxisome proliferator-activated receptor-γ (PPAR-γ) and steroid hormone receptors; the activation of these transcriptional factors modulate regulate specific patterns of genes, inducing altered responses, such as obesity. Additionally, obesogens such as BPA can induce endoplasmic reticulum (ER) stress, as an adaptive event of the preadipogenic lineage, important for adipogenic differentiation (Pu et al., 2017; Sha et al., 2009).

In the present study, the effect of chronic very low nanomolar of non-cytotoxic concentrations of Sb(III) was evaluated on adipogenesis promotion using an *in vitro* model of murine 3T3-L1 cells. These concentrations are considered very low, far from estimated detection limits of the analytical techniques used for biological sample quantification of Sb, and then underestimated from the toxicological point of view (Filella et al., 2013). In particular, the involvement of an estrogenic mechanism and of ER stress was assessed as potential mechanisms in the observed adipogenic effects of Sb.

2. Materials and methods

2.1. Chemicals

Dimethyl sulfoxide (DMSO), ethanol and isopropanol were obtained from Carlo Erba Reagent (Milan, Italy) in their highest commercially achievable purity grade. The hydrophobic polyvinylidene difluoride (PVDF) membrane, the blocking agent (non-fat dry milk powder) and the ECL plus detection kit system were purchased from Amersham Biosciences (Milan, Italy). Antimony(III) [Sb(III)] chloride ($SbCl_3$) (code #10025-91-9-100 MG) and all the other chemicals, unless otherwise indicated, were purchased from Merk Life Science (Milan, Italy).

2.2. Cell culture and treatments

3T3-L1 murine preadipocyte cells were purchased from the American Tissue Culture Collection (Manassas, VA, USA).

In preliminary experiments carried out to evaluate Sb(III) cytotoxicity, the 3T3-L1 cells were seeded in growth specific culture medium [Dulbecco's modified essential medium (DMEM) containing 10% newborn calf serum, 100 U/ml penicillin/streptomycin solution, 4 mM L-glutamine and 25 mM HEPES buffer] in 24-well plates at an initial density of 2.5×10^4 cells/well, stabilized for 24 h, and then incubated with various concentrations of Sb(III) (from 0.05 nM to 25 nM) for additional 48 h. The cells treated with the vehicle alone (DMSO 0.1 % v/v) were used as controls.

To obtain totally differentiated cells, 3T3-L1 cells were cultured in growth culture medium; to prepare 3T3-L1 monolayers, cells were seeded at 1.3×10^4 cells/cm^2 in 12-well plates and cultured for 10 days, up to the total differentiation in mature adipocytes, as described in detail in our previous work (Molonia et al., 2022). Briefly, to induce differentiation, 2-day postconfluent 3T3-L1 cells were stimulated for 4 days with 0.5 μM 3-isobutyl-1-methylxanthine, 1 μM dexamethasone and 1 μg/mL insulin in DMEM containing 10% fetal bovine serum, 100 U/ml penicillin/streptomycin solution, 4 mM L-glutamine and 25-mM HEPES buffer (MDI differentiation medium). Subsequently cells were maintained in a 10% FBS/DMEM medium containing only 1 μg/mL insulin for the remaining six days until total differentiation with a medium change at day 7. Total differentiation was reached at day 10 as evaluated by Oil Red O staining and PPAR-γ expression (data not shown). For these experiments, 3T3-L1 cells were treated, throughout all the 10 days of the differentiation process, with Sb(III) at three different concentrations (0.05, 0.5 and 5 nM). $SbCl_3$ was always freshly dissolved in DMSO and added to the cells to each medium change. The final concentration of DMSO in the culture medium during the treatments was always maintained $\leq$0.1 % (v/v). The cells treated with the vehicle alone (DMSO 0.1 % v/v) and exposed to the inducers of differentiation were used as controls. At the end of the exposure time, cells were immediately processed and/or preserved at −80 °C until the analysis required for each test.

In a series of experiments, the estrogen receptor (EsR) antagonist ICI-182,780 (ICI) at the concentration of 10 nM was added throughout the differentiation process in the presence or not of Sb(III).

2.3. Sulforhodamine B assay

The cytotoxic effect of Sb(III) on 3T3-L1 cells was assessed by sulforhodamine B assay. In detail, after the treatment, the culture medium was removed and, after washing with Dulbecco's phosphate buffered saline (DPBS), the cells were fixed for 1 h at 4 °C using 10% trichloroacetic acid (w/v). Then the dishes were air-dried and sulforhodamine B (0.4% w/v in 1% acetic acid) was added for 30 min at room temperature. After this step the unbound dye was washed out with 1% (v/v) of acetic acid and the dye caught in the cells was dissolved in 10 mM Tris base solution. Thus, the absorbance was measured at 565 nm using a microplate reader (GloMax® Discover System-TM397).

2.4. Oil Red O staining

The Sb(III) effect on intracellular lipid accumulation was measured by Oil Red O staining assay as described previously by Muscarà et al. (2019) with few modifications. Briefly, on day 10, differentiated cells were fixed for 1 h at room temperature with 4% formaldehyde and, after a wash with 60% isopropanol, stained for 10 min in agitation with Oil red O (0.3% w/v in 60% isopropanol). Then the Oil red O solution was removed and the adipogenic cultures were observed by optical microscope and photographed (40x magnification). Finally, the Oil Red O stain retained in the cells was eluted in 100% isopropanol and lipid droplets was quantified by spectrophotometric analysis at 490 nm using a microplate reader (GloMax® Discover System-TM397). Results were expressed as fold change against control.

2.5. Detection of reactive oxygen species (ROS) formation

The intracellular ROS levels were determined using the dichlorodihydro-fluorescein diacetate (DCFH-DA) as previously reported by Bashllari et al. (2023). Briefly, following treatment, the cells were washed twice with DPBS and incubated with 50 μM DCFH-DA at 37 °C for 30 min. Fluorescence values were measured at 485 nm and 530 nm (wavelength of excitation and emission, respectively) in a microplate

reader (GloMax® Discover System-TM397). The assay was performed in triplicate. ROS levels were expressed as DCFH-DA relative fluorescence intensity per mg of proteins against control.

2.6. Mitotic clonal expansion (MCE) process

When induced to differentiate, growth-arrested 3T3-L1 cellssynchronously reenter the cell cycle and undergo MCE. Since this event takes place at the early stage of preadipocyte differentiation, the cells were used at fourth day, at the end of induction step. Postconfluent 3T3-L1 cells were induced to differentiate with the addition of MDI in the presence or absence of Sb(III) (0.05-0.5-5 nM) for 4 days. Then cell count was performed by Erythrosin B exclusion test. Erythrosin B stain was prepared as a 0.1% solution in DPBS according to the manufacturer's instructions (Sigma Aldrich). After trypsinization, cell number was determined by hemocytometer counts and expressed as percentage vs control cells. Cell cycle distribution was determined by DNA staining with BD Cycletest™ Plus DNA Kit according to Allegra et al. (2018). Briefly, cells were harvested and fixed in 70% cold ethanol overnight and then nuclei collected and stained with BD Cycletest™ Plus DNA Kit. The PI fluorescence was then measured by flow cytometry (FACScan II, Becton Dickinson San Jose, CA, USA). A minimum of 30,000 cells were acquired per sample, and data were analyzed using the software Modfit 3. The percentage of cells in G0/G1, S and G2/M was determined from histograms of DNA content.

2.7. Cell lysates preparation

Following the appropriate treatments, 3T3-L1 cells were washed with DPBS and harvested with a scraper. For nuclear and cytosolic extracts, cells were incubated in a hypotonic buffer (10 mM HEPES, pH 7.9, 1.5 mM $MgCl_2$, 10 mM KCl and 5% glycerol). Nuclei were recovered by centrifugation and the supernatant was kept as the cytoplasmic extract. Nuclear proteins were then obtained by incubation with a hypertonic buffer (20 mM HEPES, 1 mM $MgCl_2$, 400 mM NaCl, 1 mM EGTA, 0.1 mM EDTA, and 10% glycerol. Total lysate was instead achieved by treating harvested cells with a lysis buffer (10 mM Tris–HCl, 1 mM EDTANa2, 150 mM NaCl, 5% glycerol, 0.1% SDS, and 1% Tryton). All lysis buffers contained protease inhibitors (1 μg/ml leupeptine, 2 μg/ml aprotinine, 1 mM benzamidine, and 5 mM NaF) and 1 mM DTT.

Protein fractions were stored at −20 °C until use. Protein concentration in lysates was determined using the Bradford method (Bradford, 1976).

2.8. Immunoblotting

For immunoblot analyses, 20 μg of nuclear lysates or 30 μg of total or cytosolic lysates were denatured in 4 × SDS-PAGE reducing sample buffer (260 mM Tris–HCl, pH 8.0, 40% (v/v) glycerol, 9.2% (w/v) SDS, 0.04% bromo-phenol blue, and 2-mercaptoethanol as reducing agent) and subjected to SDS-PAGE on 10 % or 12 % acrylamide/bisacrylamide gels. Following the separation, the proteins were transferred to PVDF membranes. The membranes were blocked, for 1 h at room temperature, with Tris-buffered saline containing 5% of lyophilized non-fat milk and then incubated overnight with specific primary antibodies: rabbit anti C/EBP-β (LAP) polyclonal antibody (#3087 Cell Signaling Technology) (1:1000), mouse anti-PPAR-γ monoclonal antibody (#sc-7273 Santa Cruz Biotechnology) (1:1500), rabbit anti–NF–κB p65 polyclonal antibody (#PA5-16545 Invitrogen) (1:1000), rabbit anti-Phospho-IKK α/β (Ser176/180) monoclonal antibody (#sc-2697 Cell Signaling Technology) (1:1000), Rabbit anti-IKKβ monoclonal antibody (#8943 Cell Signaling Technology) (1:1000), mouse anti-Cox-2 monoclonal antibody (#sc-160107 Santa Cruz Biotechnology) (1:200), rabbit anti-XBP-1s (E9V3E) monoclonal antibody (#40435 Cell Signaling Technology) (1:500), rabbit anti-Phospho-eIF2α (Ser51)(D9G8) monoclonal antibody (#3398 Cell Signaling Technology) (1:500), rabbit anti-eIF2α (D7D3) monoclonal antibody (#5324 Cell Signaling Technology) (1:1000), rabbit anti p21 Waf1/Cip1 monoclonal antibody (#sc-271610 Santa Cruz Biotechnology, Dallas, TX, USA) (1:500), rabbit anti-β-Actin monoclonal antibody (#4970 Cell Signaling Technology) (1:6000), rabbit anti-Lamin-B monoclonal antibody (#13435 Cell Signaling Technology) (1:1500), followed by 2 h incubation with peroxidase-conjugated secondary antibody HRP labeled goat antirabbit Ig (#7074 Cell Signaling Technology) (1:6000), goat anti-Mouse IgM Secondary Antibody, HRP conjugate (#7076 Cell Signaling Technology) (1:6000), and visualized with an ECL plus detection system (Amersham; GE Healthcare Life Sciences). Blots were detected using High Performance chemiluminescence film (Amersham Hyperfilm™ ECL; GE Healthcare Life Sciences. The intensities of the bands were quantified using the Image J Program and the equivalent loading of proteins in each well was confirmed by Ponceau staining, β-actin, Lamin B or total IKK and eIF2α.

2.9. Real-time PCR

Total cellular RNA was extracted using E.Z.N.A.® Total RNA kit according to manufacturer's instruction (OMEGA Bio-Tek, VWR), quantified by Quanti-iT TM RNA assay kit QUBIT (Invitrogen, Milan, Italy), and reverse transcripted with M-MLV Reverse Transcriptase. Quantitative real-time polymerase chain reaction (PCR; Applied Biosystems 7300 Real-Time PCR System, CA, USA) coupled with SYBR green chemistry (SYBR green JumpStart Taq Ready Mix) was performed for identification of mRNA levels of FASN (NM_007988) (FW 5′- GGA GGT GGT GAT AGC CGG TAT-3′, RV 5′-TGG GTA ATC CAT AGA GCC CAG-3' (Zhang et al., 2016)), FABP4 (NM_024406) (FW 5′-AAG GTG AAG AGC ATC ATA ACC CT -3′, RV 5′- TCA CGC CTT TCA TAA CAC ATT CC-3' (Molonia et al., 2023), SREBP-1 (NM_011480) (FW 5′-TGG CTT GGT GAT GCT ATG TT -3′, RV 5′- TAA GGG GTT GGG AGT AGA GG -3' (Ning et al., 2017)), MCP1 (NM_011333) (FW 5′- GGC TCA GCC AGA TGC AGT TAA -3′, RV 5′- CCT ACT CAT TGG GAT CAT CTT GCT -3' (Asano et al., 2014)), TNF (NM_013693) (FW 5′-AAG CCT GTA GCC CAC GTC GTA-3′, RV 5′-GGC ACC ACT AGT TGG TTG TCT TTG -3' (Shao et al., 2017)), IL-6 (NM_031168) (FW 5′-GAT GGA TGC TAC CAA ACT GGA T -3′, RV 5′-CCA GGT AGC TAT GGT ACT CCA GA -3' (Molonia et al., 2022)), IL-8 (NM_011339) (FW 5′- GCA CTT GGG AAG TTA ACG CA -3′, RV 5′- GCA CAG TGT CCC TAT AGC CC-3' (Liu et al., 2020)), CHOP (NM_007837) (FW 5′-CGG AAC CTG AGG AGA GAG TG-3′, RV 5′-TAT AGG TGC CCC CAA TTT CA-3' (Asano et al., 2014)), GRP78 (NM_001163434) (FW 5′-GGA TGC GGA CAT TGA AGA CT-3′, RV 5′-TCC CAA CGA AAG TTC CTG AG-3' (Asano et al., 2014)). 18S rRNA (NR_003278) (FW 5′-GTA ACC CGT TGA ACC CCA TT-3′, RV 5′-CCA TCC AAT CGG TAG TAG CG-3′) (Molonia et al., 2020) was used to normalise mRNA levels since it was identified as stable housekeeping gene in our experimental conditions. Data were elaborated by SDS 1.3.1 software (Applied Biosystems, Foster City, CA, USA) and expressed as threshold cycle (Ct). The fold increase of mRNA expression compared with MDI cells was determined using the $2^{-\Delta\Delta Ct}$ method (Molonia et al., 2020).

2.10. Statistical analysis

Experiments were performed in triplicate and repeated three times. Data are expressed as mean ± SD from three experiments and statistical analysis was carried out by a one-way ANOVA test, followed by Tukey's HSD, using the statistical software ezANOVA (https://people.cas.sc.edu/rorden/ezanova/index.html). Differences in groups and treatments were considered significant for $p < 0.05$.

3. Results

3.1. Antimony in vitro toxicity

The cytotoxic effects of Sb(III) have been firstly studied exposing 3T3-L1 cells to different concentrations for 48h and cell viability

evaluated by sulforhodamine B assay. Fig. 1 shows that Sb(III) induces significant cell death starting from 12.5 nM (cell viability <90%). For this reason, a non-cytotoxic Sb(III) concentration range starting from 0.05 to 5 nM was employed for further investigations. One has to underline that although present in relatively low concentrations in human tissues, Sb levels recovered in human blood were in the range 0.15–13.55 ng/ml (Lai et al., 2022). So, the range of Sb concentrations employed in our experiments is able to mimicking that which can be found in human circulation.

3.2. Effects of antimony on adipogenic activity

The effects of Sb(III) on adipogenesis were evaluated exposing the 3T3-L1 cells to the tested compound during the differentiation process (10 days). Oil Red O staining showed that, in our experimental conditions, Sb(III) exposure induces an increase in the size and numbers of lipid droplets compared to control cells and these effects are dose-dependent (Fig. 2A). Additionally, the extent of lipid accumulation induced by Sb(III) was 1.32 ± 0.03, 1.75 ± 0.05 and 2.33 ± 0.05 relative content *vs* control cells (respectively for 0.05, 0.5 and 5 nM) (Fig. 2B).

To better understand the molecular mechanisms involved in pro-adipogenic effect of Sb(III), the expression levels of key transcription factors and adipogenic genes involved in adipocyte differentiation were analyzed. At this aim, at the end of differentiation process, PPAR-γ protein levels and FASN, FABP4 and SREBP-1 gene expression were determined. Moreover, C/EBP-β protein levels were evaluated after the first 4 days of differentiation. The results obtained confirmed that the exposure to Sb(III) induces a marked increase in C/EBP-β and PPAR-γ levels, which are important transcription factors expressed at the early and late stage of adipocyte differentiation respectively, compared to control cells (Fig. 3A and B). In particular, these effects were dose-dependent and the lower nanomolar Sb(III) concentration was already able to activate these transcription factors.

We also examined the level of expression of FASN, FABP4 and SREBP-1 downstream genes of PPAR-γ pathway that regulate fatty acid metabolism during adipocyte differentiation. Our results confirmed their dose-dependent expression starting from 0.05 nM compared to control cells following treatment with Sb(III) (Fig. 3 C). These data all demonstrate how the effects of Sb(III) in the induction of the adipogenesis process are regulated by the activation of the critical adipogenic transcriptional factors C/EBP-β and PPAR-γ.

3.3. Antimony affects MCE process

During the stage of adipogenesis, MDI inducers initiate cell cycle in pre-adipocytes, and cells began to proliferate through a process called MCE, an early event indispensable for adipogenesis in 3T3-L1. The number of cells counted after 4 days of MDI exposure is reported in Fig. 4 A. There was a significant concentration-related trend for an increase in cell number for Sb(III); this effect, in comparison with controls, was observed starting from the lowest tested concentration.

When we analyzed the cell cycle using fluorescence-activated cell sorting, it was evident that Sb(III) changed the cell cycle distribution among different phases (G0/G1, G2/M, and S), as reported in Fig. 4 B and 4 C. In fact, compared to the control, Sb(III) exposure increased in a dose-dependent manner the percentage of cells at the G2/M phase while reducing that at G0/G1 phase. The results indicated that Sb(III) exposure might increase 3T3-L1 cell proliferation by accelerating cell cycle progression via the G2/M phase.

Literature data reported that mice lacking the cyclin-dependent kinase inhibitors such as p21 display adipose tissue hyperplasia with accelerated adipogenesis (Hallenborg et al., 2014). In our experimental conditions, Sb(III) reduced p21 protein expression in a dose-dependent way starting from the lowest concentration tested (Fig. 4 D).

3.4. Effects of the EsR antagonist ICI on antimony–induced differentiation

Given that antimony has been proven as able to modulate and interfere with estrogenic receptors activity at concentrations as low as 1 μM (Choe et al., 2003), the potential role of the EsR in Sb(III)–induced adipogenic process was investigated. Since in our experiments cell exposure to Sb(III) was demonstrated to upregulate PPAR-γ expression during adipocyte differentiation, we investigated if there is a correlation between EsR activity and the expression of this transcription factor. At this aim, 3T3-L1 cells were cotreated with Sb(III) and the EsR antagonist ICI (10 nM) during all the differentiation process and the effect on PPAR-γ levels was evaluated. ICI alone did not affect cell viability and PPAR-γ levels at the concentration used (data not shown). In our experimental conditions, the EsR antagonist ICI prevented Sb (III)-induced PPAR-γ over expression and reestablished its levels to those of control cells (Fig. 5), so suggesting that Sb(III) is able to induce 3T3-L1 cells differentiation in mature adipocyte through an EsR-mediated mechanism.

3.5. Antimony induces the NF-κB proinflammatory pathway

Adipocyte hyperplasia and hypertrophy during obesity induce increased adipose tissue inflammation involving proinflammatory adipokines release that generates a state of chronic low-grade inflammation. Activation of the inflammatory and stress-signaling networks, such as the nuclear factor-kappa B (NF-κB) pathway, is involved in these

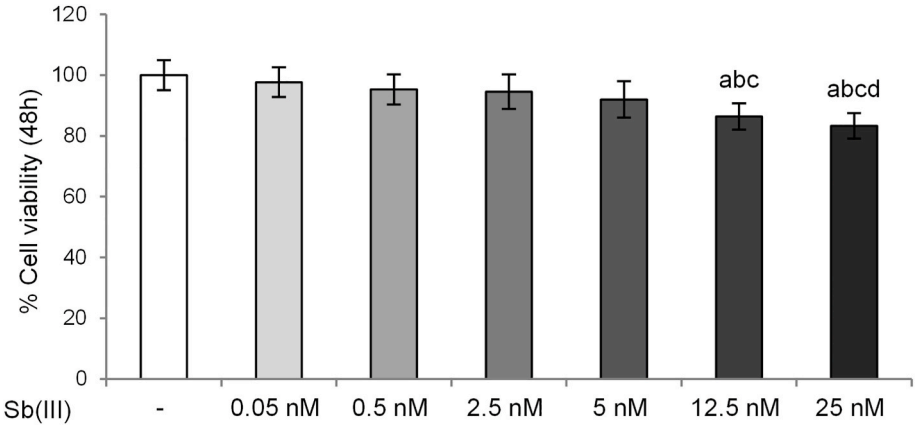

Fig. 1. Cell Viability. Cytotoxicity was evaluated by SRB assay on 3T3-L1 cells exposed to different concentrations of Sb(III) for 48 h. Control cells were treated with the vehicle (DMSO) alone. Results are expressed as mean ± S.D. of three independent experiments. [a]p < 0.05 vs control cells; [b]p < 0.05 vs Sb(III) 0.05 nM; [c]p < 0.05 vs Sb(III) 0.5 nM; [d]p < 0.05 vs vs Sb(III) 2.5 nM.

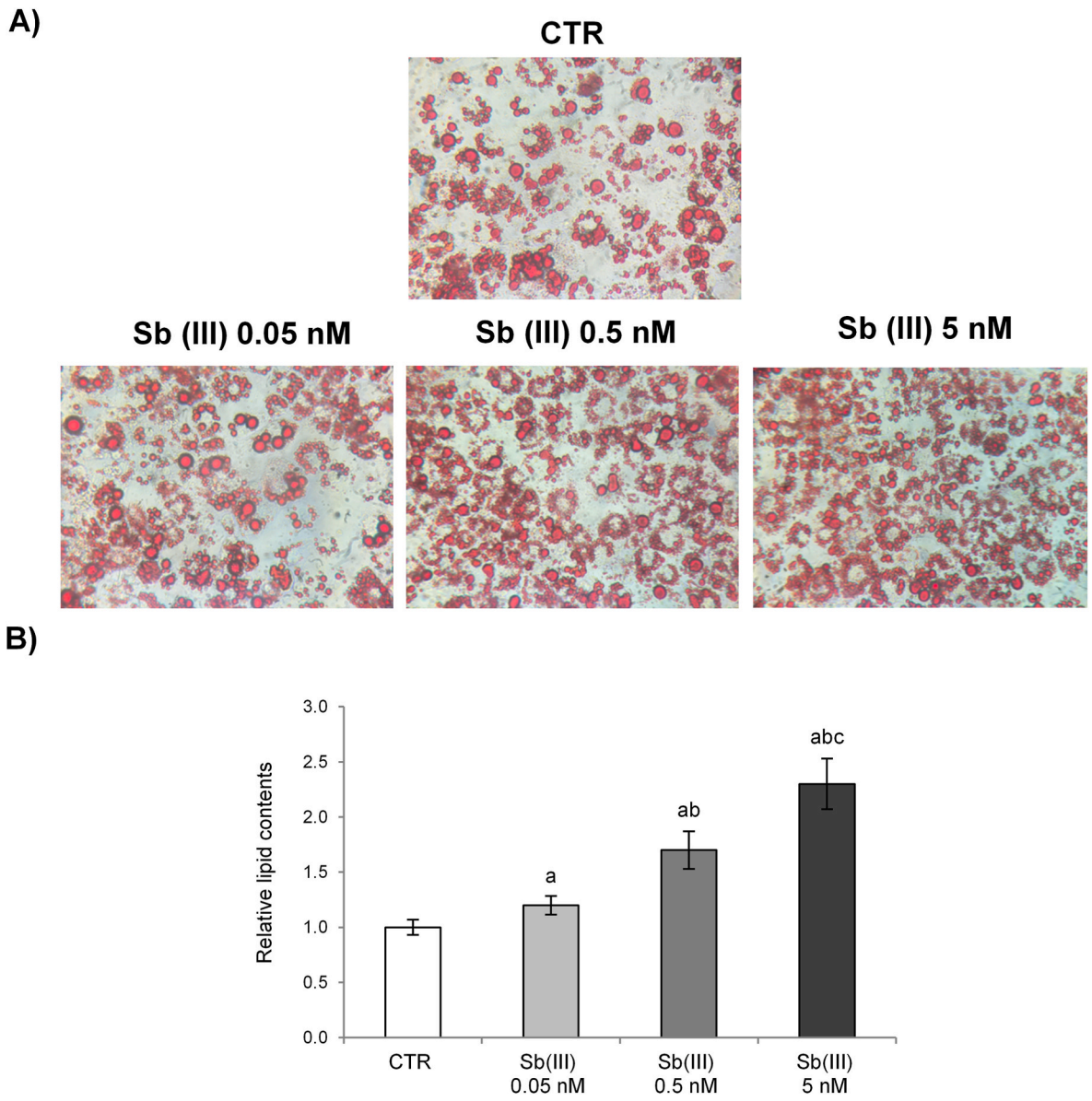

Fig. 2. Oil Red O staining. 3T3-L1 cells were cultured or not with Sb(III) (0.05, 0.5 and 5 nM) for 10 days. Cells cultured with MDI alone were used as controls (CTR). (A) Representative images of Oil red O staining of 3T3-L1 adipocytes at indicated concentration of Sb(III) (original magnification at × 40). (B) Lipids were extracted from 3T3-L1 adipocytes by using chloroform/methanol mixture and expressed as relative content vs MDI control cells; results are reported as mean ± S.D. of three independent experiments. $^{a}p < 0.05$ vs CTR; $^{b}p < 0.05$ vs Sb(III) 0.05 nM; $^{c}p < 0.05$ vs Sb(III) 0.5 nM. (For interpretation of the references to colour in this figure legend, the reader is referred to the Web version of this article.)

effects. In particular, NF-κB mediates cell proliferation and cytokines release to stimulate the immune response. NF-kB signaling cascades converge on the activation of the Inhibitor of κB kinase (IKK) complex that promotes degradation of kb-inhibitor (IkB) and release of NF-κB, which translocates to the nucleus and induces the transcription of target genes.

As reported in Fig. 6, Sb(III) induced NF-κB p65 nuclear translocation, starting from 0.05 nM, and this effect was dose-dependent. NF-κB p65 activation was associated to IKK phosphorylation confirming that Sb(III) modulates NF-κB pathway through phosphorylation of IκB by IKK. Also in this case, the effects were dose-dependent starting from the lowest Sb(III) concentration tested.

Additionally, the activation of NF-κB pathway was evaluated at transcriptional and posttranscriptional level. Sb(III) induced MCP-1, IL-6, IL-8 and TNF-α gene expression, important pro-inflammatory cytokines regulated by NF-κB, and increased the expression of COX-2 protein, the inducible COX isoform involved in prostaglandin biosynthesis and inflammation. Interestingly these data confirmed that Sb(III) was effective already at very low concentrations (0.05 nM), revealing the activation of proinflammatory machinery.

3.6. Antimony induces ER stress response

ER has pivotal roles in lipid biosynthesis, calcium ion storage, and protein processing in adipose tissue. Under particular conditions, such as increased fatty acids or environmental stressor stimuli, ER homeostasis is compromised inducing ER stress. This, in turn, activates the unfolded protein response (UPR) to restore the ER homeostasis through mechanisms involving PERK (PKR-like ER kinase), IRE1 (inositol requiring enzyme 1), and ATF6 (activating transcription factor 6), all of which are inhibited at basal states. Recent reports showed that ER stress is a central regulator connecting obesity and inflammation. In fact, ER has emerged as a critical regulator of systemic metabolic homeostasis and has been proposed as the immediate cause of chronic inflammation (Li, 2018). At

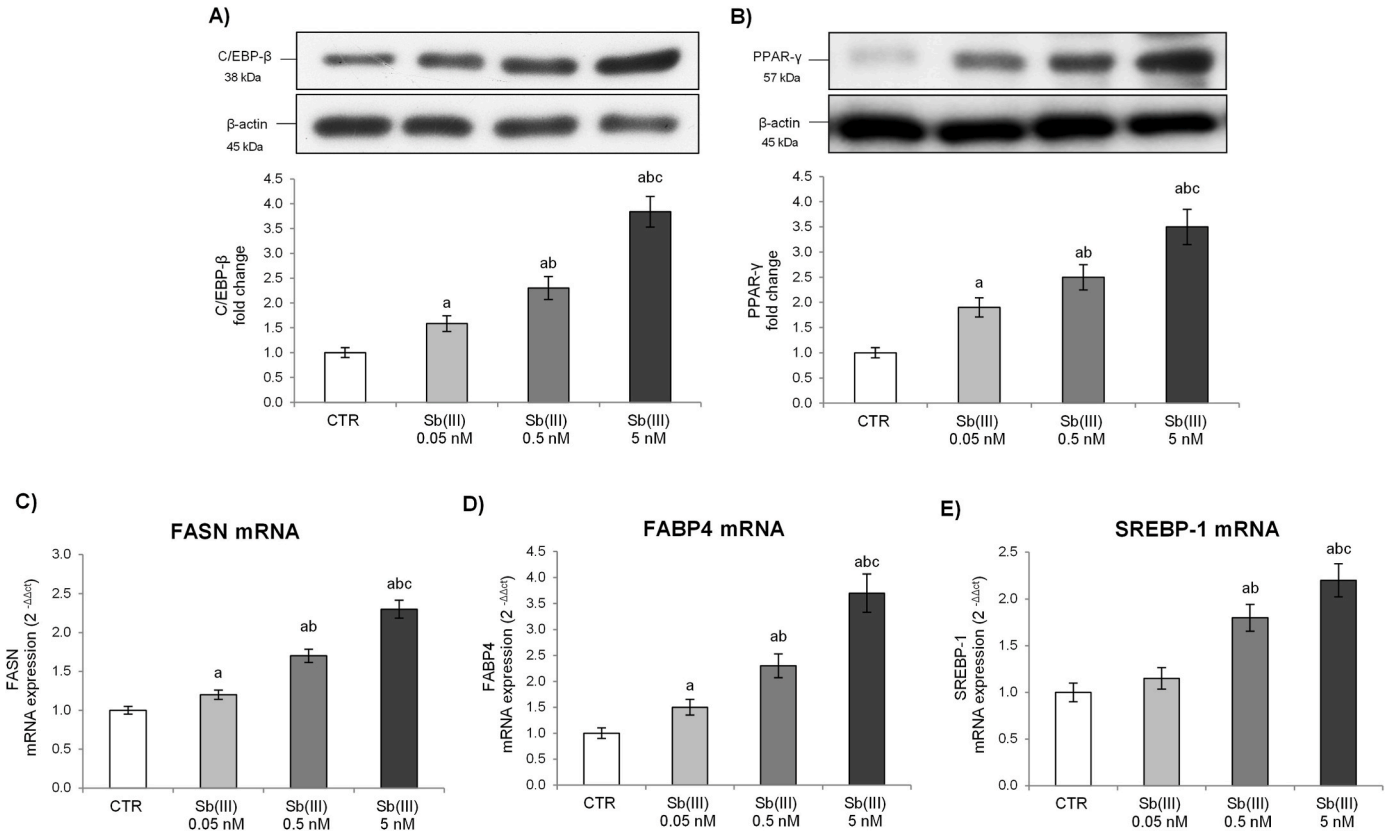

Fig. 3. Effects of antimony on adipogenic markers. 3T3-L1 preadipocytes were cultured or not with Sb(III) (0.05, 0.5 and 5 nM) for 10 days (B–E), whereas C/EBP-β levels (A) were evaluated at the end of the first 4 days of treatment with Sb(III). Cells cultured with MDI alone were used as controls (CTR). (A, B) C/EBP-β and PPAR-γ protein expression. The densitometry results are reported as fold change compared to control cells. C/EBP-β and PPAR-γ values were normalized to the corresponding β-actin value. All data are expressed as mean ± SD of three independent experiments. (C, D, E) FASN, FABP4 and SREBP-1 gene expression values are expressed as $2^{-\Delta\Delta Ct}$ and normalized against MDI cells. 18S rRNA was used as housekeeping gene. $^{a}p < 0.05$ vs CTR; $^{b}p < 0.05$ vs Sb(III) 0.05 nM; $^{c}p < 0.05$ vs Sb(III) 0.5 nM.

this aim we evaluated the capability of Sb(III) to induce ER stress in adipocytes during their differentiation by determining target proteins of UPR mechanisms such as p-eIF2α and the spliced XBP-1 (XBP-1s).

In our experimental conditions, Sb(III) exposure during the pre-adipocytes differentiation process induced XBP-1s expression in a dose-dependent way starting from the lower Sb(III) concentration 0.05 nM (Fig. 7). These data confirmed the Sb(III) role in adipocyte dysfunction since XBP1s activates the transcription of genes related to UPR, as well as of genes involved in *de novo* lipogenesis, insulin resistance, and inflammation (Wu et al., 2015). Similarly, Sb(III) induced eIF2α phosphorylation, which is involved in protein translation attenuation, protein synthesis reduction, and correction of misfolding proteins accumulation within ER lumen (Amen et al., 2019), so confirming the activation of ER stress response following adipocytes exposure to Sb(III).

The activity of UPR signaling pathways under our experimental conditions was evaluated also at transcriptional level. The spliced XBP-1s acts as a transcription factor for ER stress-related genes such as the glucose-regulated protein 78 (GRP78) gene, coding for a chaperon protein involved in protein folding (Amen et al., 2019); while p-eIF2 induces the expression of CCAAT/enhancer-binding protein homologous protein (CHOP), which is involved in apoptotic response (Vestuto et al., 2022). In our experiments, Sb(III) induced GRP78 and CHOP gene expression starting from 0.05 nM, so confirming the activation of signaling events involved in UPR response (Fig. 7 C and D).

Finally, our data also confirmed the relationship between ER stress and oxidative stress, since prolonged activation of the UPR may also alter cell redox status and cause toxic accumulation of ROS within the cells (Almanza et al., 2019). In our experimental conditions, Sb(III) exposure during adipocytes differentiation was able to induce intracellular ROS accumulation starting from 0.05 nM (Fig. 7 E).

4. Discussion

In the present study, for the first time, the proadipogenic properties of Sb during preadipocytes differentiation was demonstrated. In fact, low nanomolar Sb exposure (from 0.05 to 5 nM) induced a dose-dependent lipid accumulation compared to the control. Sb, at all the concentration tested, induced a marked increase in C/EBP-β and PPAR-γ levels, known as the master regulators of early and late phase of adipogenesis (Evseeva et al., 2021). Although Sb effect on adipocytes differentiation was not ever studied, our data let us hypothesize that this metal acts as obesogen at low nanomolar levels. However, at the same extent, other well-known obesogens like BPA and phthalates, are able to induce adipogenesis through the same mechanism (Mohajer et al., 2021).

The process of adipogenesis includes preadipocyte proliferation and adipocyte differentiation throughout which cell-cycle modulators and differentiation inducers cooperate and so produce a cascade of signals leading to preadipocyte commitment to the adipocyte phenotype. In the first step, cyclin-dependent kinase (CDKs), in combination with D-type and E-type cyclins play key roles in regulating cell progression (Naaz et al., 2004). Activities of cyclins/CDKs complex are modulated by cyclin-dependent kinase inhibitors (CDKIs), such as p21 and p27, which inactivate cyclin/CDK complexes so inhibiting the cell progression (Naaz et al., 2004). Our data demonstrate that Sb stimulated pre-adipocytes proliferation inducing G2/M phase of cell cycle exiting from

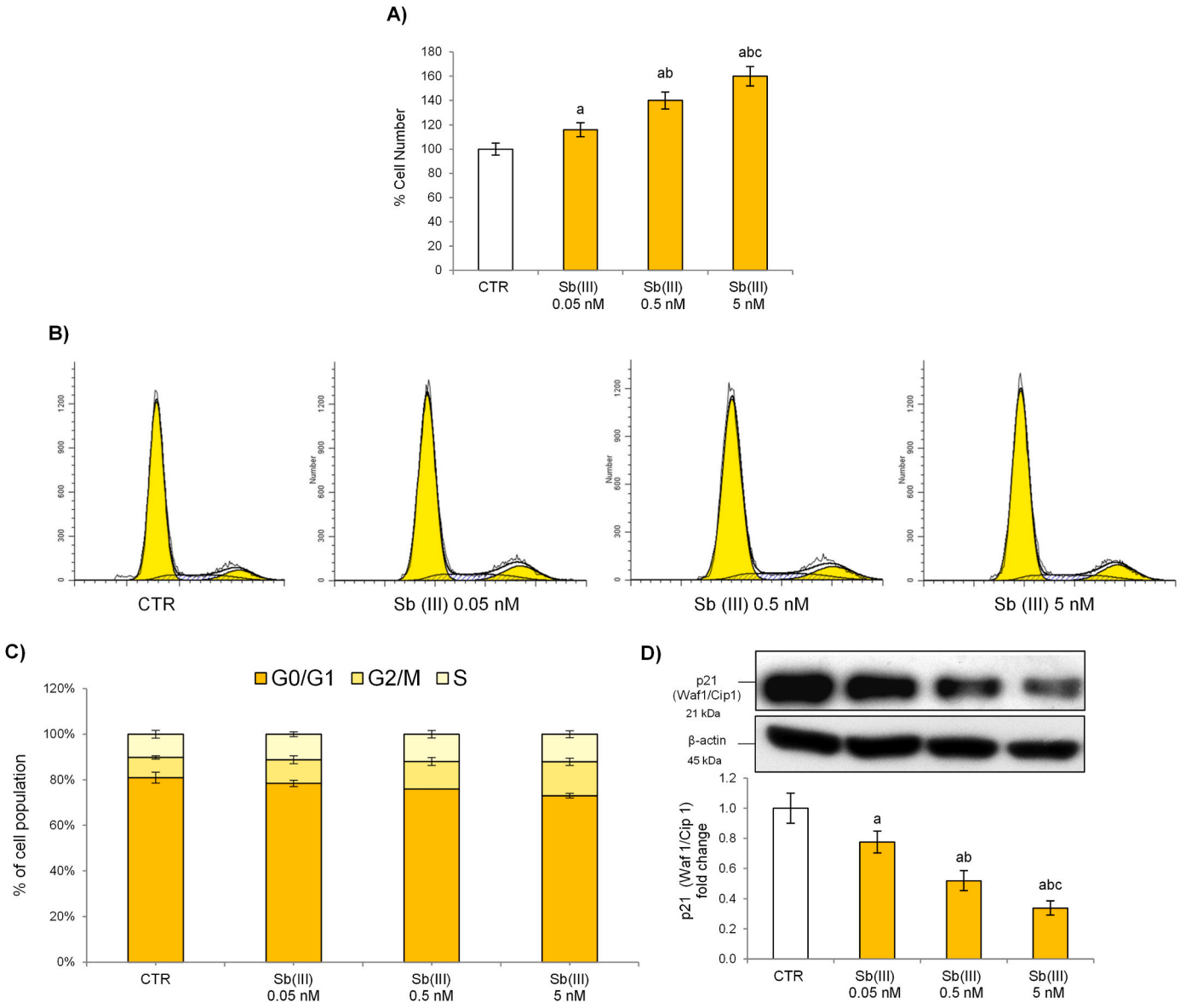

Fig. 4. Effects of antimony on mitotic clonal expansion in 3T3-L1 cells. 3T3-L1 cells were cultured or not with Sb(III) (0.05, 0.5 and 5 nM) from day 0 to day 4. Cells treated with MDI alone were used as controls (CTR). (A) Effect on cell number: cell count (reported as mean ± SD of three independent experiments) was determined after trypsinization on day 4 by hemocytometer counts. (B–C) Effect on cell cycle arrest: The number of cells in G0/G1, G2/M and S at day 4 was determined from histograms of DNA content and expressed as mean percentages of total cells ± SD of three independent experiments. (D) Effect on p21 (Waf1/Cip1) protein expression: the densitometric results are reported as fold change compared to control cells; p21 value was normalized to the corresponding β-actin value. $^{a}p < 0.05$ vs CTR; $^{b}p < 0.05$ vs Sb(III) 0.05 nM; $^{c}p < 0.05$ vs Sb(III) 0.5 nM.

G0/G1 phase and this effect was associated to reduced cell-cycle inhibitor p21. In fact, it has been reported that p27 and p21 decrease at the beginning of MCE in 3T3-L1 preadipocytes, while cessation of MCE is accompanied by an increase of both CDKIs (Morrison and Farmer, 1999).

Moreover, several other intracellular targets and pathways have been reported as potential modulator of adipogenesis, often acting in a gender-specific manner (Casals-Casas and Desvergne, 2011). For example, BPA showed to bind to several receptors and to act as an estrogen receptor modulator through classical and non-classical estrogenic pathways (Boucher et al., 2014; Ohlstein et al., 2014) and, similarly to estradiol (E2), BPA induced the expression of C/EBP-β, PPARγ and other adipocyte-specific genes such as FAS and leptin in 3T3-L1 (Phrakonkham et al., 2008). Recent data indicates that estrogens play a role in the adipose environment where estradiol is a major regulator of adipocytes precursors proliferation via EsR-dependent obesogenic mechanism leading to adipocyte hyperplasia (Saavedra-Peña et al., 2023). Heavy metals and metalloids, such as Sb, may have estrogenic activity, suggesting that they act not only as generalized toxicants but also as endocrine disruptors (Kabir et al., 2015). Our data demonstrated that Sb (III) modulates adipogenesis through activation of the EsR. In fact, when an EsR pharmacological inhibitor was used, Sb was unable to induce PPAR-γ expression, having this effect been demonstrated also for other obesogens (Boucher et al., 2014). Low dose BPA can promote estrogen-like activities through rapid responses via non-classical estrogen pathways (Alonso-Magdalena et al., 2012) and these effects can be reverted by the EsR antagonist ICI (Boucher et al., 2014). However, these data need further investigation in order to better comprehend the exact mechanism involving the direct or indirect EsR targeting.

In addition to these metabolic dysfunctions, we demonstrated the activation of proinflammatory response after Sb exposure. The activation of the proinflammatory transcription factor NF-kB was observed

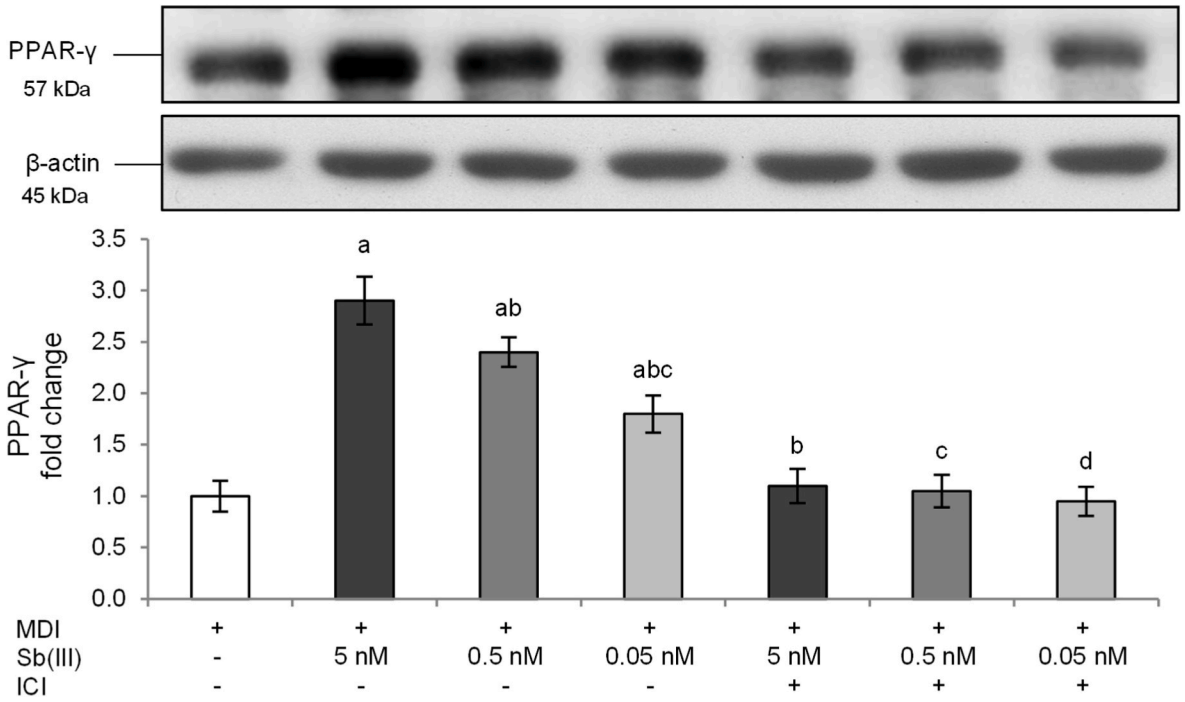

Fig. 5. Effect of the EsR antagonist ICI on Sb(III) induced PPAR-γ overexpression. 3T3–L1 preadipocytes were cultured in MDI containing Sb(III) (0.05, 0.5 and 5 nM) with or without ICI 10 nM for 10 days. Cells treated with MDI alone were used as controls. The densitometry results are reported as fold change compared to MDI cells. PPAR-γ protein values were normalized to the corresponding β-actin values. All data are expressed as mean ± SD of three independent experiments. $^{a}p < 0.05$ vs MDI control cells; $^{b}p < 0.05$ vs Sb(III) 5 nM; $^{c}p < 0.05$ vs Sb(III) 0.5 nM; $^{d}p < 0.05$ vs Sb(III) 0.05 nM.

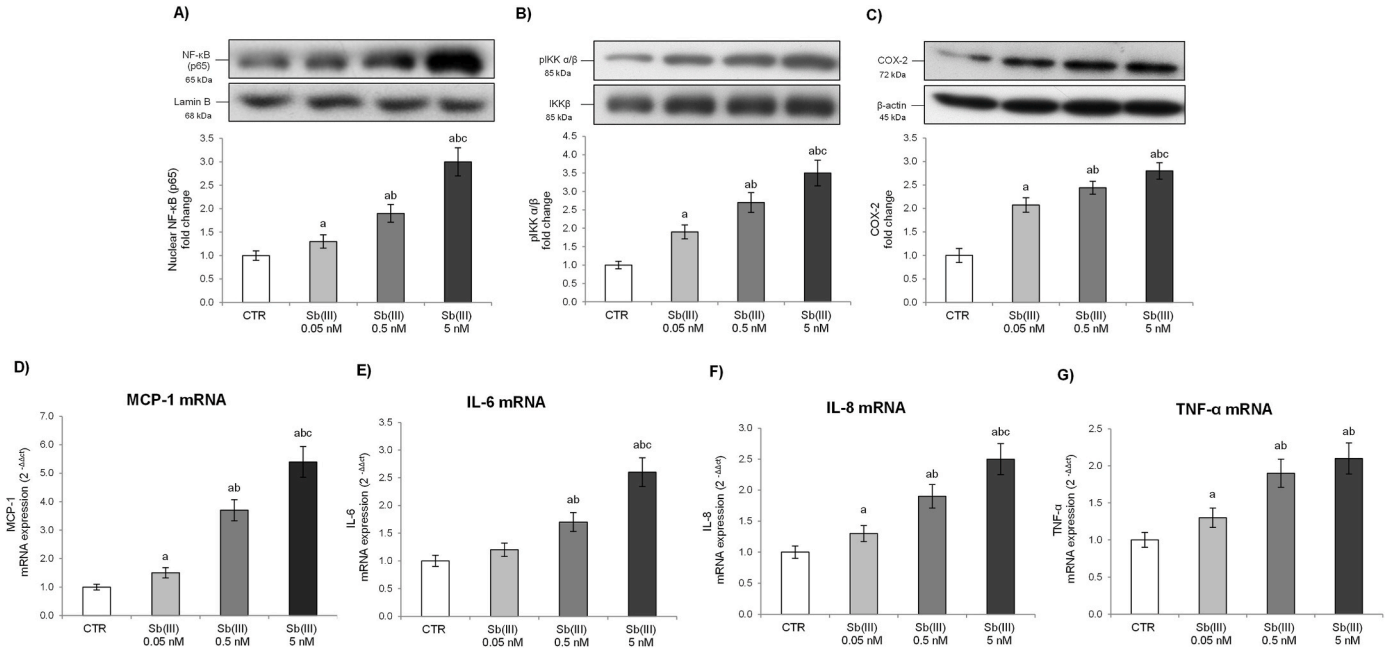

Fig. 6. Effects of antimony on NF-κB **pathway**. 3T3–L1 preadipocytes were cultured in MDI containing or not Sb(III) (0.05, 0.5 and 5 nM) for 10 days. Cells treated with MDI alone were used as controls (CTR). (A, B, C) NF-κB p65, pIKK and COX-2 protein expression. The densitometry results are reported as fold change compared to MDI cells. Levels of lamin-B, IKK and β-actin were used as loading control. All data are expressed as mean ± SD of three independent experiments. (D, E, F, G) MCP-1, IL-6, IL-8 and TNF-α gene expression values are expressed as $2^{-\Delta\Delta Ct}$ and normalized against MDI cells. 18S rRNA was used as housekeeping gene. $^{a}p < 0.05$ vs CTR; $^{b}p < 0.05$ vs Sb(III) 0.05 nM; $^{c}p < 0.05$ vs Sb(III) 0.5 nM.

already at the 0.05 nM concentration with a dose-dependent effect. Sb also induced NF-kB transcriptional and post-transcriptional response affecting MCP-1 and COX-2 expression. EDCs have been demonstrated to elevate inflammatory responses that in turn affect adipocyte function and, ultimately, adaptation to metabolic demands. In particular, EDCs-induced inflammation is supposed to be an important mechanism in metabolic dysfunction. For example, BPA exposure in adolescent C57BL/6J mice induced proinflammatory cytokines, chronic low-grade inflammation, and increased body weight and fat (Yang et al., 2016). Similarly, BPA proinflammatory effects have also been evidenced *in vitro*

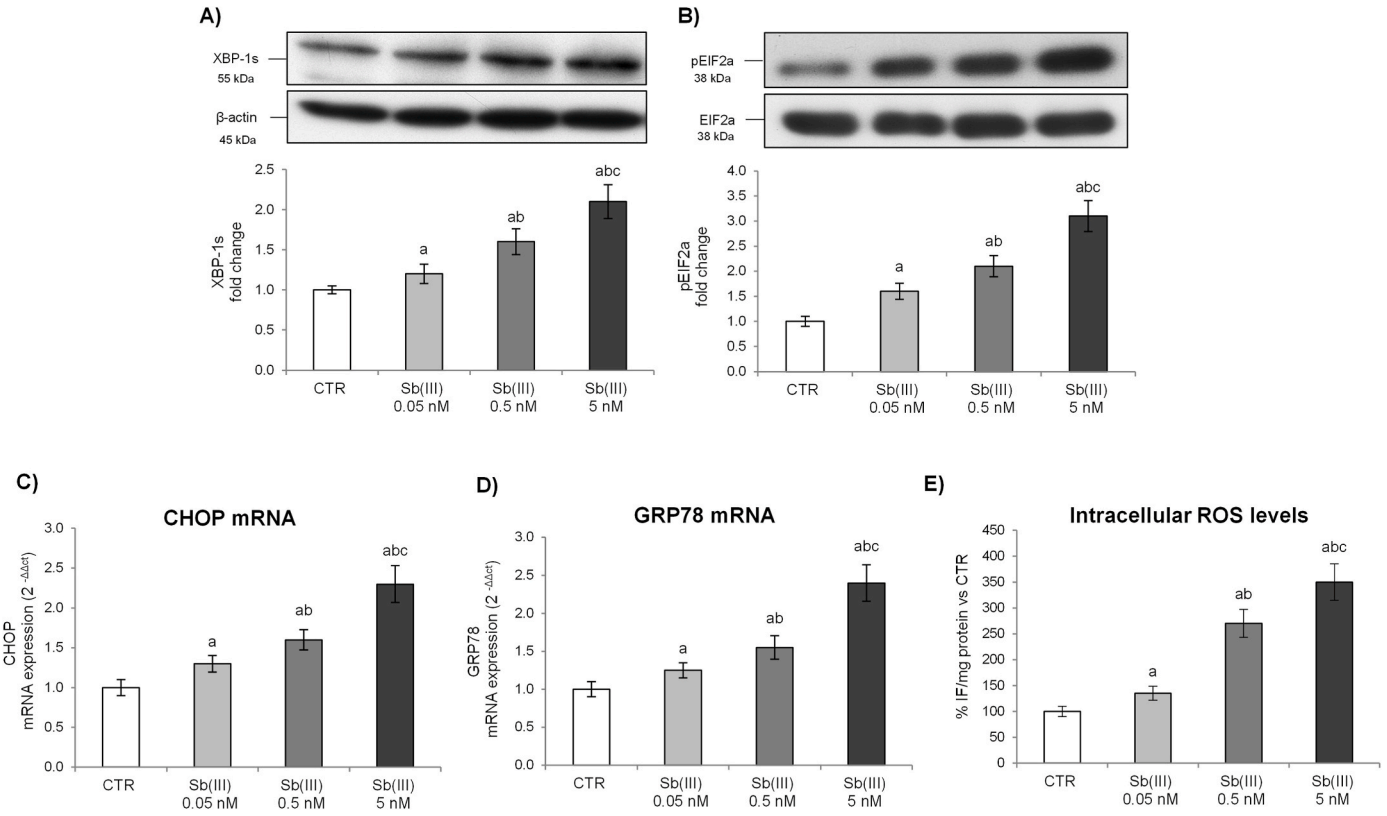

Fig. 7. Effects of antimony on ER stress pathway. 3T3–L1 preadipocytes were cultured in MDI containing or not Sb(III) (0.05, 0.5 and 5 nM) for 10 days. Cells treated with MDI alone were used as controls (CTR). (A, B) XBP-1s and pEIF2a protein expression. Densitometry results are reported as fold change compared to MDI cells. Levels of β-actin and EIF2a were used as loading control. (C,D) CHOP and GRP78 mRNA expression values are expressed as $2^{-\Delta\Delta Ct}$ and normalized against MDI cells. 18S rRNA was used as housekeeping gene. (E) Intracellular ROS levels are reported as % change of fluorescence intensity/mg of proteins against control. All data are expressed as mean ± SD of three independent experiments. [a]$p < 0.05$ vs CTR; [b]$p < 0.05$ vs Sb(III) 0.05 nM; [c]$p < 0.05$ vs Sb(III) 0.5 nM.

with increased pro-inflammatory cytokine secretion in murine adipocytes, supporting a contribution to the development of systemic low-grade inflammation (Ariemma et al., 2016).

Recent studies have pointed out that the ER stress is a core signaling for the inflammation. The ER is considered a main source of ROS and considered a sensor of metabolic stress, extensively associated with inflammatory responses. Under some circumstances, such as increased fatty acids, destruction the ER homeostasis induces signaling pathway called UPR, which in turn can also activate the inflammatory response pathway via regulation of gene transcription and protein synthesis (Kawasaki et al., 2012). Intrauterine exposure of mice to low-dose of the environmental EDC dibutyl phthalate showed to promote obesity in offspring via ER stress (Li et al., 2020). In our experimental conditions, higher levels of ROS were detected after Sb(III) exposure during preadipocytes differentiation. This effect was associated to ER stress activation, since the UPR markers XBP-1s and pEIF2a were upregulated by Sb(III) in a dose-dependent way. Additionally, our data demonstrated that also UPR downstream markers, such as Grp78 and CHOP, were upregulated at the same extent by Sb(III) exposure during preadipocytes differentiation. Although ER stress is considered a common molecular pathway for the main pathogenic mechanisms of obesity (Cnop et al., 2012), the molecular mechanisms linking EDCs, ER and obesity are still lacking (Kim et al., 2022). Evidence supports a role for EDCs as a trigger for ER stress even if further studies are needed to confirm this assumption (Kim et al., 2022).

5. Conclusion

The present results all support evidences suggesting adverse effects of Sb(III) low doses on adipose tissue. Sb(III) exposure during preadipocytes differentiation induces increase in lipid accumulation through different mechanisms such as cell cycle modulation, EsR activation and ER stress response. However, this study has the typical limitations of *in vitro* tests and is based on a single murine cell line so that further studies are needed to confirm these *in vitro* data on *in vivo* models. Nevertheless our findings contribute to remark that, in the actual context of endemic metabolic disorders, and giving that mixtures of chemicals with common biological endpoints (such as EDCs) can act additively (Ribeiro et al., 2017), any action oriented towards the reduction of the use and diffusion of these compounds is now crucial.

CRediT authorship contribution statement

Maria Sofia Molonia: Validation, Formal analysis, Investigation, Writing – original draft, preparation, Visualization. **Claudia Muscarà:** Investigation. **Antonio Speciale:** Conceptualization, Methodology, Validation, Formal analysis, Resources, Writing – original draft, preparation, Writing – review & editing, Visualization. **Federica Lina Salamone:** Formal analysis, Investigation, Visualization. **Gregorio Costa:** Formal analysis, Investigation. **Grazia Vento:** Formal analysis, Investigation. **Antonella Saija:** Antonella Saija, Resources, Writing – review & editing, All authors have read and agreed to the published version of the manuscript. **Francesco Cimino:** Conceptualization, Methodology, Resources, Writing – original draft, preparation, Writing – review & editing, Visualization, Supervision, Project administration.

Declaration of competing interest

The authors declare that they have no known competing financial interests or personal relationships that could have appeared to influence

the work reported in this paper.

Data availability

Data will be made available on request.

References

Allegra, A., Speciale, A., Molonia, M.S., Guglielmo, L., Musolino, C., Ferlazzo, G., Costa, G., Saija, A., Cimino, F., 2018. Curcumin ameliorates the in vitro efficacy of carfilzomib in human multiple myeloma U266 cells targeting p53 and NF-kappaB pathways. Toxicol. Vitro 47, 186–194. https://doi.org/10.1016/j.tiv.2017.12.001.

Almanza, A., Carlesso, A., Chintha, C., Creedican, S., Doultsinos, D., Leuzzi, B., Luís, A., McCarthy, N., Montibeller, L., More, S., Papaioannou, A., Püschel, F., Sassano, M.L., Skoko, J., Agostinis, P., de Belleroche, J., Eriksson, L.A., Fulda, S., Gorman, A.M., Healy, S., Kozlov, A., Muñoz-Pinedo, C., Rehm, M., Chevet, E., Samali, A., 2019. Endoplasmic reticulum stress signalling - from basic mechanisms to clinical applications. FEBS J. 286, 241–278. https://doi.org/10.1111/febs.14608.

Alonso-Magdalena, P., Ropero, A.B., Soriano, S., García-Arévalo, M., Ripoll, C., Fuentes, E., Quesada, I., Nadal, Á., 2012. Bisphenol-A acts as a potent estrogen via non-classical estrogen triggered pathways. Mol. Cell. Endocrinol. 355, 201–207. https://doi.org/10.1016/j.mce.2011.12.012.

Amen, O.M., Sarker, S.D., Ghildyal, R., Arya, A., 2019. Endoplasmic reticulum stress activates unfolded protein response signaling and mediates inflammation, obesity, and cardiac dysfunction: therapeutic and molecular approach. Front. Pharmacol. 10, 977. https://doi.org/10.3389/fphar.2019.00977.

Ariemma, F., D'Esposito, V., Liguoro, D., Oriente, F., Cabaro, S., Liotti, A., Cimmino, I., Longo, M., Beguinot, F., Formisano, P., Valentino, R., 2016. Low-dose bisphenol-A impairs adipogenesis and generates dysfunctional 3T3-L1 adipocytes. PLoS One 11, e0150762. https://doi.org/10.1371/journal.pone.0150762.

Asano, H., Kanamori, Y., Higurashi, S., Nara, T., Kato, K., Matsui, T., Funaba, M., 2014. Induction of beige-like adipocytes in 3T3-L1 cells. J. Vet. Med. Sci. 76, 57–64. https://doi.org/10.1292/jvms.13-0359.

Bashllari, R., Molonia, M.S., Muscarà, C., Speciale, A., Wilde, P.J., Saija, A., Cimino, F., 2023. Cyanidin-3-O-glucoside protects intestinal epithelial cells from palmitate-induced lipotoxicity. Arch. Physiol. Biochem. 129, 379–386. https://doi.org/10.1080/13813455.2020.1828480.

Boreiko, C.J., Rossman, T.G., 2020. Antimony and its compounds: health impacts related to pulmonary toxicity, cancer, and genotoxicity. Toxicol. Appl. Pharmacol. 403, 115156 https://doi.org/10.1016/j.taap.2020.115156.

Boucher, J.G., Boudreau, A., Atlas, E., 2014. Bisphenol A induces differentiation of human preadipocytes in the absence of glucocorticoid and is inhibited by an estrogen-receptor antagonist. Nutr. Diabetes 4, e102. https://doi.org/10.1038/nutd.2013.43.

Bradford, M.M., 1976. A rapid and sensitive method for the quantitation of microgram quantities of protein utilizing the principle of protein-dye binding. Anal. Biochem. 72, 248–254. https://doi.org/10.1006/abio.1976.9999.

Brandsma, S.H., Leonards, P.E.G., Koekkoek, J.C., Samsonek, J., Puype, F., 2022. Migration of hazardous contaminants from WEEE contaminated polymeric toy material by mouthing. Chemosphere 294, 133774. https://doi.org/10.1016/j.chemosphere.2022.133774.

Casals-Casas, C., Desvergne, B., 2011. Endocrine disruptors: from endocrine to metabolic disruption. Annu. Rev. Physiol. 73, 135–162. https://doi.org/10.1146/annurev-physiol-012110-142200.

Choe, S.Y., Kim, S.J., Kim, H.G., Lee, J.H., Choi, Y., Lee, H., Kim, Y., 2003. Evaluation of estrogenicity of major heavy metals. The Science of the total environment 312, 15–21. https://doi.org/10.1016/s0048-9697(03)00190-6.

Cnop, M., Foufelle, F., Velloso, L.A., 2012. Endoplasmic reticulum stress, obesity and diabetes. Trends Mol. Med. 18, 59–68. https://doi.org/10.1016/j.molmed.2011.07.010.

Darbre, P.D., 2006. Metalloestrogens: an emerging class of inorganic xenoestrogens with potential to add to the oestrogenic burden of the human breast. J. Appl. Toxicol. : JAT 26, 191–197. https://doi.org/10.1002/jat.1135.

Darbre, P.D., 2017. Endocrine disruptors and obesity. Current obesity reports 6, 18–27. https://doi.org/10.1007/s13679-017-0240-4.

Evseeva, M.N., Balashova, M.S., Kulebyakin, K.Y., Rubtsov, Y.P., 2021. Adipocyte biology from the perspective of in vivo research: review of key transcription factors. Int. J. Mol. Sci. 23 https://doi.org/10.3390/ijms23010322.

Filella, M., 2020. Antimony and PET bottles: checking facts. Chemosphere 261, 127732. https://doi.org/10.1016/j.chemosphere.2020.127732.

Filella, M., Belzile, N., Chen, Y.-W., 2013. Human exposure to antimony. IV. Contents in human blood. Crit. Rev. Environ. Sci. Technol. 43, 2071–2105. https://doi.org/10.1080/10643389.2013.790741.

Hallenborg, P., Petersen, R.K., Feddersen, S., Sundekilde, U., Hansen, J.B., Blagoev, B., Madsen, L., Kristiansen, K., 2014. PPARγ ligand production is tightly linked to clonal expansion during initiation of adipocyte differentiation. J. Lipid Res. 55, 2491–2500. https://doi.org/10.1194/jlr.M050658.

Kabir, E.R., Rahman, M.S., Rahman, I., 2015. A review on endocrine disruptors and their possible impacts on human health. Environ. Toxicol. Pharmacol. 40, 241–258. https://doi.org/10.1016/j.etap.2015.06.009.

Kawasaki, N., Asada, R., Saito, A., Kanemoto, S., Imaizumi, K., 2012. Obesity-induced endoplasmic reticulum stress causes chronic inflammation in adipose tissue. Sci. Rep. 2, 799. https://doi.org/10.1038/srep00799.

Kim, K., Kwon, J.S., Ahn, C., Jeung, E.B., 2022. Endocrine-disrupting chemicals and their adverse effects on the endoplasmic reticulum. Int. J. Mol. Sci. 23 https://doi.org/10.3390/ijms23031581.

La Merrill, M.A., Vandenberg, L.N., Smith, M.T., Goodson, W., Browne, P., Patisaul, H.B., Guyton, K.Z., Kortenkamp, A., Cogliano, V.J., Woodruff, T.J., Rieswijk, L., Sone, H., Korach, K.S., Gore, A.C., Zeise, L., Zoeller, R.T., 2020. Consensus on the key characteristics of endocrine-disrupting chemicals as a basis for hazard identification. Nat. Rev. Endocrinol. 16, 45–57. https://doi.org/10.1038/s41574-019-0273-8.

Lai, Z., He, M., Lin, C., Ouyang, W., Liu, X., 2022. Interactions of antimony with biomolecules and its effects on human health. Ecotoxicol. Environ. Saf. 233, 113317 https://doi.org/10.1016/j.ecoenv.2022.113317.

Li, H., Li, J., Qu, Z., Qian, H., Zhang, J., Wang, H., Xu, X., Liu, S., 2020. Intrauterine exposure to low-dose DBP in the mice induces obesity in offspring via suppression of UCP1 mediated ER stress. Sci. Rep. 10, 16360 https://doi.org/10.1038/s41598-020-73477-3.

Li, J., Zheng, B., He, Y., Zhou, Y., Chen, X., Ruan, S., Yang, Y., Dai, C., Tang, L., 2018. Antimony contamination, consequences and removal techniques: a review. Ecotoxicol. Environ. Saf. 156, 125–134. https://doi.org/10.1016/j.ecoenv.2018.03.024.

Li, X., 2018. Endoplasmic reticulum stress regulates inflammation in adipocyte of obese rats via toll-like receptors 4 signaling. Iranian J. Basic Med. Sci. 21, 502–507. https://doi.org/10.22038/ijbms.2018.27346.6674.

Liu, C., Wang, J., Wei, Y., Zhang, W., Geng, M., Yuan, Y., Chen, Y., Sun, Y., Chen, H., Zhang, Y., Xiong, M., Li, Y., Zheng, L., Huang, K., 2020. Fat-specific knockout of Mecp2 upregulates slpi to reduce obesity by enhancing browning. Diabetes 69, 35–47. https://doi.org/10.2337/db19-0502.

Lou, Y., Ma, C., Liu, Z., Shi, J., Zheng, G., Zhang, C., Zhang, Z., 2021. Antimony exposure promotes bladder tumor cell growth by inhibiting PINK1-Parkin-mediated mitophagy. Ecotoxicol. Environ. Saf. 221, 112420 https://doi.org/10.1016/j.ecoenv.2021.112420.

Mohajer, N., Du, C.Y., Checkcinco, C., Blumberg, B., 2021. Obesogens: how they are identified and molecular mechanisms underlying their action. Front. Endocrinol. 12, 780888 https://doi.org/10.3389/fendo.2021.780888.

Molonia, M.S., Muscarà, C., Speciale, A., Salamone, F.L., Toscano, G., Saija, A., Cimino, F., 2022. The p-phthalates terephthalic acid and dimethyl terephthalate used in the manufacture of PET induce in vitro adipocytes dysfunction by altering adipogenesis and thermogenesis mechanisms. Molecules 27. https://doi.org/10.3390/molecules27217645.

Molonia, M.S., Occhiuto, C., Muscarà, C., Speciale, A., Bashllari, R., Villarroya, F., Saija, A., Cimino, F., Cristani, M., 2020. Cyanidin-3-O-glucoside restores insulin signaling and reduces inflammation in hypertrophic adipocytes. Arch. Biochem. Biophys. 691, 108488 https://doi.org/10.1016/j.abb.2020.108488.

Molonia, M.S., Salamone, F.L., Muscarà, C., Costa, G., Vento, G., Saija, A., Speciale, A., Cimino, F., 2023. Regulation of mitotic clonal expansion and thermogenic pathway are involved in the antiadipogenic effects of cyanidin-3-O-glucoside. Front. Pharmacol. 691 https://doi.org/10.3389/fphar.2023.1225586.

Morrison, R.F., Farmer, S.R., 1999. Role of PPARgamma in regulating a cascade expression of cyclin-dependent kinase inhibitors, p18(INK4c) and p21(Waf1/Cip1), during adipogenesis. J. Biol. Chem. 274, 17088–17097. https://doi.org/10.1074/jbc.274.24.17088.

Muscarà, C., Molonia, M.S., Speciale, A., Bashllari, R., Cimino, F., Occhiuto, C., Saija, A., Cristani, M., 2019. Anthocyanins ameliorate palmitate-induced inflammation and insulin resistance in 3T3-L1 adipocytes. Phytother Res. : PTR 33, 1888–1897. https://doi.org/10.1002/ptr.6379.

Naaz, A., Holsberger, D.R., Iwamoto, G.A., Nelson, A., Kiyokawa, H., Cooke, P.S., 2004. Loss of cyclin-dependent kinase inhibitors produces adipocyte hyperplasia and obesity. Faseb. J. : Off. Pub. Federat. Am. Soc. Exp. Biol. 18, 1925–1927. https://doi.org/10.1096/fj.04-2631fje.

Ning, C., Li, G., You, L., Ma, Y., Jin, L., Ma, J., Li, X., Li, M., Liu, H., 2017. MiR-185 inhibits 3T3-L1 cell differentiation by targeting SREBP-1. Biosci. Biotechnol. Biochem. 81, 1747–1754. https://doi.org/10.1080/09168451.2017.1347485.

Ohlstein, J.F., Strong, A.L., McLachlan, J.A., Gimble, J.M., Burow, M.E., Bunnell, B.A., 2014. Bisphenol A enhances adipogenic differentiation of human adipose stromal/stem cells. J. Mol. Endocrinol. 53, 345–353. https://doi.org/10.1530/jme-14-0052.

Phrakonkham, P., Viengchareun, S., Belloir, C., Lombès, M., Artur, Y., Canivenc-Lavier, M.C., 2008. Dietary xenoestrogens differentially impair 3T3-L1 preadipocyte differentiation and persistently affect leptin synthesis. J. Steroid Biochem. Mol. Biol. 110, 95–103. https://doi.org/10.1016/j.jsbmb.2008.02.006.

Pu, Y., Gingrich, J.D., Steibel, J.P., Veiga-Lopez, A., 2017. Sex-specific modulation of fetal adipogenesis by gestational bisphenol A and bisphenol S exposure. Endocrinology 158, 3844–3858. https://doi.org/10.1210/en.2017-00615.

Ribeiro, E., Ladeira, C., Viegas, S., 2017. EDCs mixtures: a stealthy hazard for human health? Toxics 5. https://doi.org/10.3390/toxics5010005.

Saavedra-Peña, R.D.M., Taylor, N., Flannery, C., Rodeheffer, M.S., 2023. Estradiol cycling drives female obesogenic adipocyte hyperplasia. Cell Rep. 42, 112390 https://doi.org/10.1016/j.celrep.2023.112390.

Saerens, A., Ghosh, M., Verdonck, J., Godderis, L., 2019. Risk of cancer for workers exposed to antimony compounds: a systematic review. Int. J. Environ. Res. Publ. Health 16. https://doi.org/10.3390/ijerph16224474.

Sha, H., He, Y., Chen, H., Wang, C., Zenno, A., Shi, H., Yang, X., Zhang, X., Qi, L., 2009. The IRE1alpha-XBP1 pathway of the unfolded protein response is required for adipogenesis. Cell Metabol. 9, 556–564. https://doi.org/10.1016/j.cmet.2009.04.009.

Snedeker, S.M., 2014. Antimony in food contact materials and household plastics: uses, exposure, and health risk considerations. In: Snedeker, S.M. (Ed.), Toxicants in Food

Packaging and Household Plastics: Exposure and Health Risks to Consumers. Springer London, London, pp. 205–230.

Vestuto, V., Di Sarno, V., Musella, S., Di Dona, G., Moltedo, O., Gomez-Monterrey, I.M., Bertamino, A., Ostacolo, C., Campiglia, P., Ciaglia, T., 2022. New frontiers on ER stress modulation: are TRP channels the leading actors? Int. J. Mol. Sci. 24 https://doi.org/10.3390/ijms24010185.

Wu, R., Zhang, Q.H., Lu, Y.J., Ren, K., Yi, G.H., 2015. Involvement of the IRE1α-XBP1 pathway and XBP1s-dependent transcriptional reprogramming in metabolic diseases. DNA Cell Biol. 34, 6–18. https://doi.org/10.1089/dna.2014.2552.

Yang, M., Chen, M., Wang, J., Xu, M., Sun, J., Ding, L., Lv, X., Ma, Q., Bi, Y., Liu, R., Hong, J., Ning, G., 2016. Bisphenol A promotes adiposity and inflammation in a nonmonotonic dose-response way in 5-week-old male and female C57BL/6J mice fed a low-calorie diet. Endocrinology 157, 2333–2345. https://doi.org/10.1210/en.2015-1926.

Zhang, C., Li, P., Wen, Y., Feng, G., Liu, Y., Zhang, Y., Xu, Y., Zhang, Z., 2018. The promotion on cell growth of androgen-dependent prostate cancer by antimony via mimicking androgen activity. Toxicol. Lett. 288, 136–142. https://doi.org/10.1016/j.toxlet.2018.02.021.

Zhang, Y., Yu, H., Gao, P., Chen, J., Yu, C., Zong, C., Lu, S., Li, X., Ma, X., Liu, Y., Wang, X., 2016. The effect of growth hormone on lipid accumulation or maturation in adipocytes. Cell. Physiol. Biochem. 39, 2135–2148. https://doi.org/10.1159/000447909.